MICRO-WAXS STUDY OF STRUCTURAL HETEROGENEITY IN SINGLE PAN-PRECURSOR AND SUBSEQUENT CARBON FIBER

C. Creighton[1], P. Lynch[1 2], S. Nunna[1], B. Fox[3] M. de Jong[4], S. Mudie[4]
e-mail: claudia.creighton@deakin.edu.au

[1]Carbon Nexus, Institute for Frontier Materials, Deakin University, Geelong, Australia
[2] CSIRO, Manufacturing Flagship, Geelong, Australia
[3] Swinburne University of Technology, Faculty of Science, Engineering and Technology, Hawthorn, Melbourne VIC 3122 Australia
[4] Australian Synchrotron, 800 Blackburn Rd, Clayton, Victoria, Australia

ABSTRACT

The crystallographic orientation distribution and micro-voids in polyacrylonitrile (PAN) based carbon fiber play a key role in controlling the fiber's strength and modulus. The evolution of microstructure from polyacrylonitrile (PAN) precursor fibers throughout oxidation and subsequent carbon fiber, processed using a 100 ton carbon fiber pilot line (Carbon Nexus, Deakin University), was studied by synchrotron wide angle X-ray scattering (WAXS). A dedicated fiber testing capability has been developed on the X-ray Fluorescence Microscopy beamline at the Australian synchrotron facility, where spatially resolving measurements (Micro-WAXS patterns) were recorded as each single fiber was translated across the focused incident X-ray probe in 1 micron steps. Probing along the lateral fiber direction, (100) and (002) WAXS patterns for the PAN and subsequent carbon fibers respectively revealed a non-uniform distribution of crystallographic properties - quantified in terms of the lattice d-spacing, crystallite size and crystallographic orientation, indicating a skin-core-structure.

1 INTRODUCTION

Carbon fibers from polyacrylonitrile (PAN) precursor are widely used in composite applications due to their high strength and modulus. Even though a significant amount of effort has been devoted to the development of high-performance carbon fibers, the strength of carbon fiber is still ten times less than its theoretical strength. The fundamental structure of carbon fibers is suggested to be an amalgamation of crystallographic micro-structures connected by an amorphous phase and nano-pores [1]. Although the method of production of carbon fibers has been well established over the past five decades, the gap between theoretical and practical property values remains enormous. Based on the carbon-carbon bond strength, the theoretical tensile strength of the carbon fibers is approximately 180 GPa. The reason for the difference in strength are structural heterogeneity and imperfections like flaws and voids that are acting as crack initiators. It is recognized that the development of micro-structure during the manufacture of carbon fibers play a critical role in

SAMPE Conference Proceedings. Charlotte, NC, May 20-23, 2019. Society for the Advancement of Material and Process Engineering – North America.

defining its final properties [1-3]. However, little efforts have been put forward to understand the structural development at the required length scale at each stage of carbon fiber manufacturing.

In the past, research was conducted to identify the micro-structural evolution in fibers from each stage of carbon fiber manufacturing [4-6]. However, the studies were conducted on a fiber bundle, where it is almost impossible to separate the effect of fiber orientation on the crystallite orientation leading to inconsistencies in the analysis. To address this issue, in the recent past, researchers [7] were able to use synchrotron X-ray facilities to extract substantial information on the transformation of micro-structure from PAN precursor to carbon fiber monofilaments. Although this was a significant development in the field of carbon fiber analysis, there has been an increased interest in defining the structural heterogeneity in the fiber cross-section. Recently, with the advancement in technology, scientists were capable to generate an X-ray beam size in the order of nanometres which facilitated the extraction of cross-sectional micro-structural information of ~7 μm carbon fibers [8-10]. While this significant breakthrough in technology was utilised to understand the influence of high temperature treatment or tension on the crystallographic evolution in the cross-section of commercial carbon fibers, the role the PAN precursor microstructure plays on the structural evolution in the resultant carbon fibers is not well understood.
Therefore, in the current work, we attempt to demonstrate how the inbuilt PAN precursor structure derived in the spinning process affects the evolution of structure in carbon fibers by studying the crystallographic microstructure development in PAN fiber cross section until its conversion to carbon fiber manufactured using a commercial carbon fiber manufacturing line. Results are presented for the crystallographic evolution of the lattice d-spacing, crystallographic orientation and crystallite size.

2 EXPERIMENTATION

2.1 Materials and processing

Carbon fiber used in this study was manufactured at Carbon Nexus, Deakin University (Australia) on an industrial scale carbon fiber pilot plant that is equipped with the latest processing technology (Despatch Industries, USA; Furnace Engineering Pty Ltd, Australia). This high-precision facility is optimized for the production of commercial grade carbon fiber at industrial scale- the order of 110 ton per annum. A schematic of the manufacturing plant and relative sample positions studied for this work are shown in Figure 1.

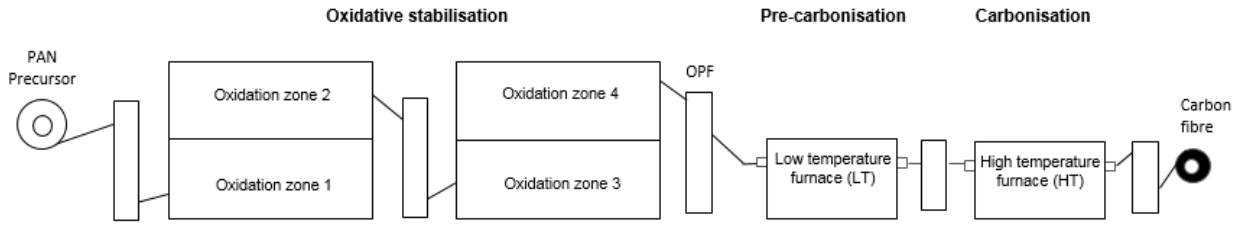

Figure 1. Schematic of the carbon fiber manufacturing plant at Carbon Nexus with sample positions, PAN precursor, OPF and final Carbon fiber.

The precursor fibers used in this study were 24k PAN fibers (Blue star Ltd, China). The PAN precursor was stabilized in oxidation ovens at temperatures between 230-260 °C. A fiber sample was then collected after stabilization, named oxidized PAN fiber (OPF). After further processing through the low temperature (LT) and high-temperature (HT) furnaces the final carbon fiber (CF) was obtained. With a line speed of 120m/h, the residence time in the stabilization ovens were 90min, and 2.5min and 2.3min in the LT and HT furnaces.

2.2 Fiber bulk properties

The tensile strength and modulus were tested using a single fiber tensile tester, Favimat (Textechno, Germany) with a 200cN load cell with a gauge length of 20 mm and a pretension of 0.5 N. Due to the variation in properties of fibers from precursor to carbon fiber, different testing conditions were applied. While the carbon fiber filaments were tested at a speed of 1 mm/min, the precursor and oxidized PAN fiber were tested at 10 mm/min according to ASTM D 3822-07. From each sample 50 filaments were analysed. The fiber diameter was measured by optical image analysis, where fibers were embedded in epoxy resin and polished. The density of the samples was obtained using a helium Ultrapyc 1200e pycnometer (Quantachrome Instruments). Physical and mechanical properties of all tested fibers are listed in Table 1.

Table 1. Physical and mechanical properties of fibers throughout the manufacturing process

	PAN Precursor	**Oxidized PAN fiber**	**Carbon Fiber**
Density (g/m^3)	1.19	1.34	1.78
Tensile Strength (MPa)	594	364	3255
Tensile Modulus (GPa)	11.4	9.9	243
Fiber Diameter (μm)	13.25	11.54	7.98

2.3 WAXS Experimentation

Small Angle X-ray Scattering (SAXS) and Wide Angle X-ray Scattering (WAXS) monofilament fiber measurements were conducted on two different beamlines at the Australian synchrotron facility. To probe the overall single fiber macroscopic properties the SAXS-WAXS beamline was employed. Fibers were mounted in the horizontal direction and SAXS-WAXS patterns were recorded for each fiber based on an incident beam probe size of ~150(V) μm x 250(H) μm with an energy of 18 keV. In this geometry, the SAXS-WAXS data for each fiber is the average signal, i.e. the entire fiber diameter x 250 μm along the fiber axis is bathed within the incident probe. For the spatially resolving SAXS-WAXS measurements the Micro- XRF beamline was used. A 2D detector was mounted downstream of the Kirkpatrick-Baez X-ray focussing optics (focal spot size ~1.5 μm^2). The experimental set-up is shown in Figure 2. Spatially resolving measurements (Micro-SAXS/Micro-WAXS patterns) were recorded as each fiber was translated across the focused incident X-ray probe in 1 μm steps. An incident beam energy of 17.5 keV and a sample to detector distance of 255 mm was used for optimum strain sensitivity (d-spacing measurements).

A schematic illustration of the spatially resolving X-ray scattering experiment is illustrated in Figure 2.

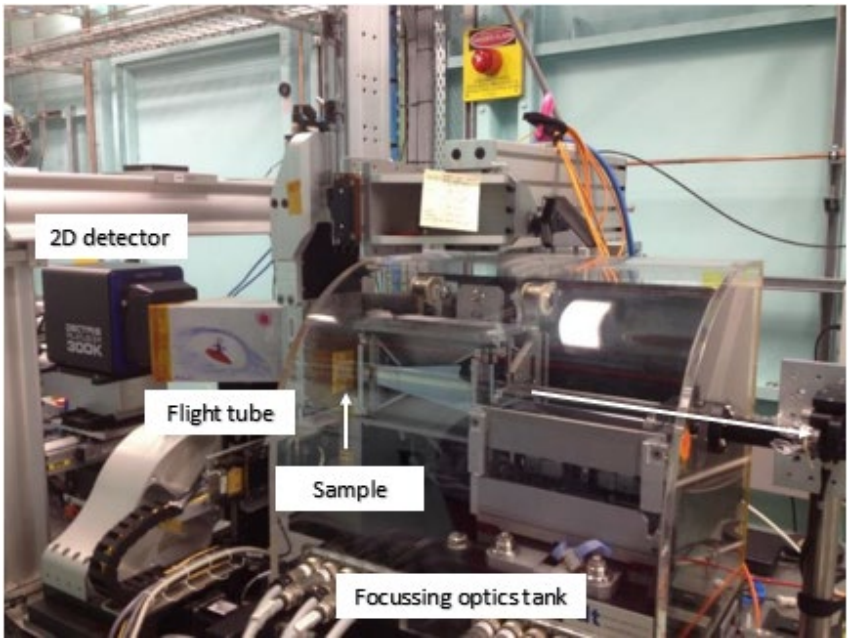

Figure 2. Experimental set-up for micro-SAXS/micro-WAXS measurements at the XRF beamline at the Australian Synchrotron

2.4 WAXS data analysis

Wide angle scattering analysis (WAXS) was performed using the line profile analysis software Topas. The WAXS patterns of all fibers investigated show different scattering pattern in the equatorial direction due to its structural transformation from a semi-crystalline polymer to a graphitic structure. Hence, for the precursor and OPF the (100) plane was analysed, while carbon fiber structure is associated with the (002) plane as demonstrated in Figure 3.

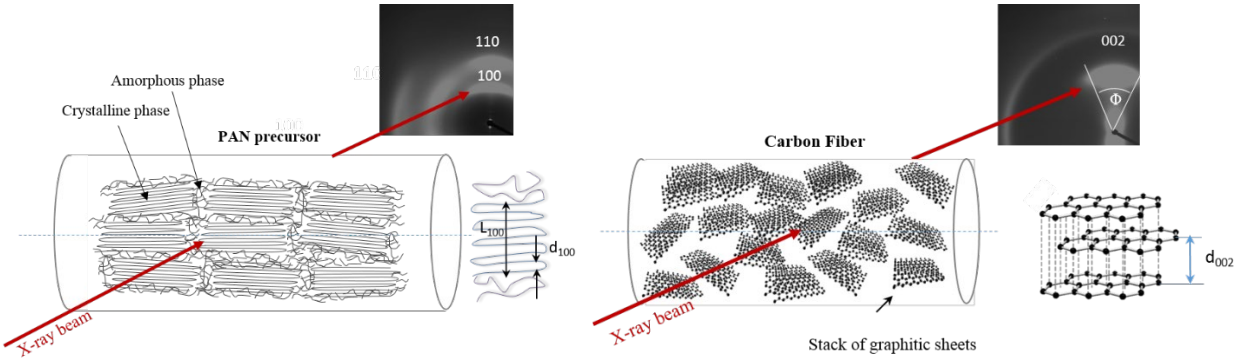

Figure 3. Schematic of microscopic structure of PAN precursor and carbon fiber and associated scattering from (100) and (002) planes, respectively.

In order to calculate the lattice spacing, *d*, the intensity distribution as a function of the diffraction angle 2θ (radial integration) is analysed. Knowing the peak position and the wavelength λ, the lattice spacing *d* is defined by use of Bragg's law.

$$\lambda = 2d * sin\theta \quad [1]$$

The apparent crystallite size (L_c) was calculated for each sample using Scherrer's equation, where K is a constant which is 0.89, λ is the wavelength of X-rays, B is the full width at half maximum intensity at 2θ (i.e., ~19° for the single filament studies and ~6.1° for fibers probed in the lateral direction),

$$L_c = \frac{K\,\lambda}{B\,\cos\theta}. \quad [2]$$

The intensity distribution as a function of the azimuthal angle φ is used to determine the orientation of the crystalline structure within the fiber. In order to evaluate the orientation perpendicular to the fiber axis, the full width half maximum of the azimuthal integration was analysed and expressed as an orientation parameter, *f*. While an orientation factor of $f = 1$ implies perfect orientation of the crystalline structures within the fibers, an orientation factor of $f = 0$ implies an isotropic distribution.

$$f = 1 - \frac{3}{2} * < sin^2(\varphi) \quad [3]$$

3 RESULTS

3.1 Single fiber structural properties

In Figure 3, the WAXS patterns of the monofilaments from each stage of the manufacturing process show a strong scattering pattern in the equatorial direction for all samples. In case of PAN fibers the micro-structure is associated with the crystallographic planes (100) with a d-spacing of ~ 4.6 Å, (110) with a d-spacing of ~3 Å and a diffuse scattering with d-spacing of ~ 3.3 Å which is associated with the amorphous regions [7, 11]. After thermal stabilization the sharp scattering related to crystallographic planes (100) and (110) appeared to diffuse and simultaneously a diffuse pattern associated with a d-spacing of ~3 Å seems to strengthen. These transformations are attributed to the evolution of ladder structures with a simultaneous annihilation of the ordered regions in the original precursor [12]. Further after the carbonization process, a strong scattering associated with the crystallographic plane (002) with a d-spacing of ~3.5 Å is observed and which is related to the development of turbostratic graphitic structure in carbon fibers [13].

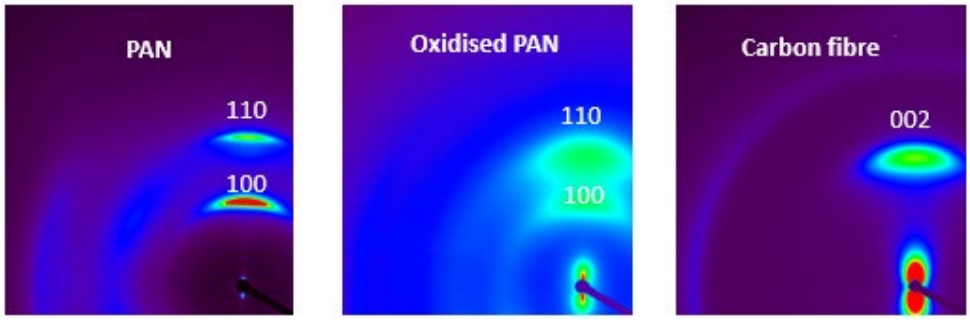

Figure 4 WAXS patterns of monofilaments from each stage of the manufacturing process

The dramatic change in fiber properties from PAN precursor to carbon fiber (Table 1) can be explained by a complete transformation of crystallographic structure (from (100) to (002)) from the oxidation to the carbonization stage as shown in Table 2. First, a decrease in crystallite size with a loss of ordered structure and simultaneous increase in d-spacing can be observed. Interestingly, the overall orientation of ordered regions in fibers was not significantly influenced during thermal stabilization, which explains the negligible variation in tensile modulus of precursor and stabilized fibers.

Table 2. Crystallographic characteristics of investigated fibers, mono-filament results

Fiber Sample	**Crystallite size, L_c (nm)**	**d-spacing (Å)**	**f**
PAN precursor	13.43	4.56	0.68
OPF	10.65	4.67	0.40
Carbon fiber	2.01	3.52	0.44

During the conversion of OPF to CF, a new crystallographic micro-structure associated with crystal plane (002) evolved with the formation of planar structures due to the process of intermolecular crosslinking between ladder structures. These planner structures stacked in the form of crystallites are caused by π-π interactions. The apparent crystallite size is ~2.0 nm and d-spacing is ~3.52 Å. The formation of these structures strengthen the back bone of carbon fibers and increase the tensile strength. Moreover, the orientation of these crystallites might have improved during thermal treatment which further influenced the tensile modulus and improved the stiffness in carbon fibers.

3.2 Micro-WAXS

Figures 4 and 5 depict the crystallographic microstructure comparison between monofilament data from WAXS (dashed lines) and spatially resolved data from micro-WAXS. Both data sets show that the crystallite size decreases from PAN to oxidized fibers, which is associated with the gradual

demolition of PAN micro-structure and evolution of a much finer graphitic structure during the carbonization process. The overall crystallite size ranges from 14.87 nm for the precursor to 1.91 nm for carbon fibers.

The spatially resolved data of PAN precursor manifests that there is a clear difference between the apparent crystallite size in the skin and the core. The skin of PAN possesses a higher crystallite size in the order of ~ 14-15nm whereas core has an apparent crystallite size of ~ 12-13 nm. Similarly, the d-spacing of skin region is approximately ~ 4.653 Å whereas the core of PAN exhibits a d-spacing of ~ 4.636 Å. Based on these observations a clear structural heterogeneity already exists in the precursor fiber, as a result of possible imbalance between the process parameters during precursor fiber manufacture. Further processing the fiber leads to a decrease in overall apparent crystallite size (from ~ 10.9 nm to ~ 7.6 nm), while the gradient from the skin to the core of OPF fibers remains similar to the precursor.

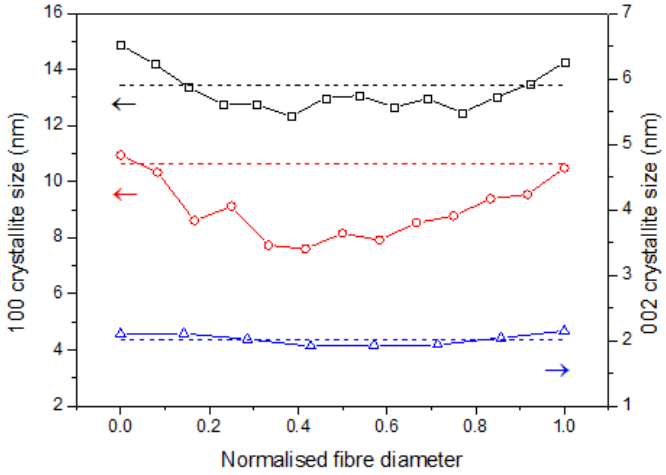

Figure 5. Variation in crystallite size across the fiber diameter precursor (black), OPF (red), carbon fiber (blue). Horizontal lines represent the results from the monofilament X-ray scattering measurements.

The overall d-spacing of OPF fibers is higher than the PAN fibers (Figure 5) which is associated with the stabilization reactions of PAN molecules during thermal stabilization [14] and tension applied. Unlike the precursor fiber, the spatially resolved data of the OPF fiber showed almost consistent d-spacing of approximately ~ 4.67 Å. Crystallites formed in the 002 plane after structural transformation from OPF to carbon fiber are significantly smaller, in the order of ten compared to OPF fibers. A much smaller, but still decreasing trend was observed in the apparent crystallite size from ~ 2.11 nm to ~ 1.91 nm from the skin to the core of carbon fibers. Although the reduction in crystallite size toward the fiber center is relatively small, the influence of PAN structure on the structural evolution in subsequent fibers throughout the manufacturing process is evident. When analyzing the d-spacing results, no clear correlation between cross-sectional heterogeneity of precursor, OPF and carbon fiber can be observed.

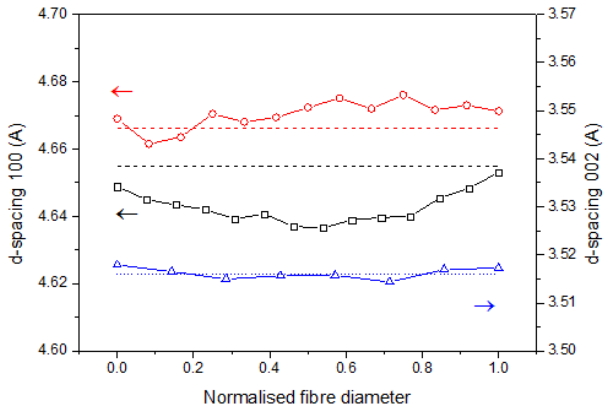

Figure 6. Variation in d-spacing across the fiber diameter precursor (black), OPF (red), carbon fiber (blue).

Figure 6 depicts the orientation of crystallites along the fiber cross section. A significant difference in orientation factor between the skin and the core of the precursor and OPF fiber is evident. The much higher orientation towards the skin of the fiber can be explained by the higher shear forces closer to the fiber surface during the spinning process. After stabilization, the alignment of crystallites along the fiber axes reduces dramatically by almost 40%. Although tension is applied during the stabilization process, the alignment of PAN crystallites constrained in the fiber is lost due to relaxation of polymer chains during heat treatment. The heterogeneity of microstructural orientation along the fiber cross-section exists to the same extent as in the precursor, where the skin possesses a higher orientation factor compared to the core. After carbonization, the microstructural orientation across the fiber are shown to be much more uniform. The formation of planer structures combined with π-π interactions between the layers in the presence of high temperatures could have led to homogeneity in the microstructure orientation in the cross section of carbon fibers.

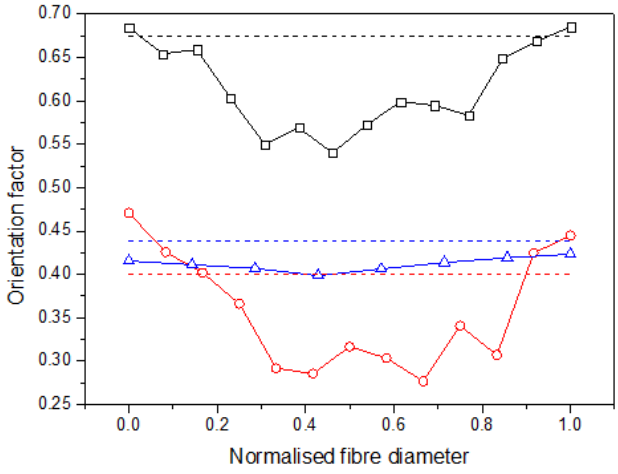

Figure 7. Variation in fiber orientation across the fiber diameter precursor (black), OPF (red), carbon fiber (blue).

4 CONCLUSIONS

Scanning synchrotron micro X-ray diffraction of was conducted on single fibers to map the heterogeneity of cross-sectional micro-structure of PAN-based carbon fiber during carbon fiber production. It can be said that in most cases the skin, which represents the larger fiber volume, and its properties agree with and determine the overall mono-filament properties. The results indicate that the skin-core micro-structure identified in the initial PAN fiber was retained through-out the fiber processing path and culminated with a carbon fiber that retains the skin-core effect. Comparing the tensile properties of PAN precursor and resultant carbon fiber it is evident that in order to have high tensile properties the arrangement and strong connection between the crystallites are key factors to be considered rather than the size of crystallites.

5 REFERENCES

[1] Kobayashi, T., Sumiya, K., Fujii, Y., Fujie, M., Takahagi, T., Tashiro, K. "Stress-induced microstructural changes and crystallite modulus of carbon fiber as measured by X-ray scattering", *Carbon* 50(3) (2012) 1163-1169. https://doi.org/10.1016/j.carbon.2011.10.029

[2] F. Liu, F., Wang, H., Xue, L., Fan, L., Zhu, Z. "Effect of microstructure on the mechanical properties of PAN-based carbon fibers during high-temperature graphitization", *Journal of Materials Science* 43(12) (2008) 4316-4322.

[3] Liu, X., Zhu, C., Guo, J., Liu, Q., Dong, H., Gu,Y., Liu, R., Zhao, N., Zhang, Z., Xu, J. "Nanoscale dynamic mechanical imaging of the skin–core difference: From PAN precursors to carbon fibers", *Materials Letters* 128(0) (2014) 417-420. https://doi.org/10.1016/j.matlet.2014.04.176

[4] Yu, M.-J., Wang, C.-G., Bai, Y.-J., Wang, Y.-X., Zhu, B. "Evolution of tension during the thermal stabilization of polyacrylonitrile fibers under different parameters" *Journal of Applied Polymer Science*, 102 (2006), pp. 5500-5506. https://doi.org/10.1002/app.23960

[5] Ko, T.H. "Influence of continuous stabilization on the physical properties and microstructure of PAN-based carbon fibers" *Journal of Applied Polymer Science*, 42 (1991), pp. 1949-1957. https://doi.org/10.1002/app.1991.070420719

[6] Fu, Z., Gui, Y., Cao, C., Liu, B., Zhou, C., Zhang, H. "Structure evolution and mechanism of polyacrylonitrile and related copolymers during the stabilization", *Journal of Materials Science* 49(7) (2014) 2864-2874.

[7] Dalton, H., Heatley, F., Budd, P.M. "Thermal stabilization of polyacrylonitrile fibers", *Polymer* 40(20) (1999) 5531-5543. https://doi.org/10.1016/S0032-3861(98)00778-2

[8] Kobayashi, T., Sumiya, K., Fujii, Y., Fujie, M., Takahagi, T., Tashiro, K. "Stress concentration in carbon fiber revealed by the quantitative analysis of X-ray crystallite modulus and Raman peak shift evaluated for the variously-treated monofilaments under constant tensile forces", *Carbon* 53(0) (2013) 29-37. https://doi.org/10.1016/j.carbon.2012.10.012

[9] Kobayashi, T., Sumiya, Fukuba, Y., M. Fujie, M., Takahagi, T., Tashiro, K. "Structural heterogeneity and stress distribution in carbon fiber monofilament as revealed by synchrotron micro-beam X-ray scattering and micro-Raman spectral measurements", *Carbon* 49(5) (2011) 1646-1652.

[10] Loidl, D., Paris, O., Rennhofer, H., Müller, M., Peterlik, H. "Skin-core structure and bimodal Weibull distribution of the strength of carbon fibers", *Carbon* 45(14) (2007) 2801-2805.

[11]Liu, W.R. X. D. “X-ray studies on the structure of polyacrylonitrile fibers”, *Macromolecules* 26(12) (1993) 3030-3036. https://doi.org/10.1016/j.carbon.2007.09.011
[12]Arbab, S., Mirbaha, H., Zeinolebadi, A., Nourpanah, P. “Indicators for evaluation of progress in thermal stabilization reactions of polyacrylonitrile fibers”, *Journal of Applied Polymer Science* 131(11) (2014) DOI: 10.1002/APP.40343. https://doi.org/10.1002/app.40343
[13]Zhu, C. Liu, X., Mao, Y. Liu, R., Zhao, N., Zhang, X., Xu, J. 2D SAXS/WAXD analysis of PAN carbon fibre microstructure in organic/inorganic transformation”, *Chinese Journal of Polymer Science* (CJPS) 31(5) (2013) 823-832.
[14]Yu, M.-J., Bai, Y.-J., Wang, C.-G., Xu, Y., Guo, P.-Z. “A new method for the evaluation of stabilization index of polyacrylonitrile fibers”, *Materials Letters* 61(11-12) (2007) 2292-2294. https://doi.org/10.1016/j.matlet.2006.08.071